

See discussions, stats, and author profiles for this publication at: <https://www.researchgate.net/publication/270802427>

Segmented Kinetic Investigation on Condensed KCl Sulfation in SO₂/O₂/H₂O at 523–1023 K

ARTICLE *in* ENERGY & FUELS · NOVEMBER 2014

Impact Factor: 2.79

READS

37

1 AUTHOR:



Xuebin Wang

Xi'an Jiaotong University

47 PUBLICATIONS 239 CITATIONS

[SEE PROFILE](#)

Segmented Kinetic Investigation on Condensed KCl Sulfation in SO₂/O₂/H₂O at 523–1023 K

Zhongfa Hu, Xuebin Wang,* Zhao Wang, Yibin Wang, and Houzhang Tan

MOE Key Laboratory of Thermo-Fluid Science and Engineering, Xi'an Jiaotong University, Xi'an 710049, China

ABSTRACT: Sulfation of condensed alkali chloride significantly affects deposition and corrosion in heat transfer surfaces during biomass combustion. This study investigates the heterogeneous sulfation of condensed potassium chloride (KCl) in a fixed-bed reactor at 523–1023 K with levels of 0.1–2% sulfur oxide (SO₂), 2.5–10% oxygen (O₂), and 5–15% water vapor. The sulfation rate is determined by measuring the sulfur content in solid residues. No other potassium species are found, and potassium sulfate (K₂SO₄) is the only sulfation product. The KCl sulfation within the temperature range of 523–1023 K was divided into three stages: (1) slow sulfation rate increase below 723 K, (2) slight decline at 723–773 K, and (3) rapid increase over 823 K. The sulfation mechanism transformation occurs between 723 and 823 K. This change in the reaction mechanism is further proven by investigating the effects of SO₂ and O₂ reactants and water vapor at 723 and 923 K. The KCl–K₂SO₄ mixture forms a eutectic to change the reaction mode at high temperatures, thereby explaining the phenomenon, which is further confirmed by the results of scanning electron microscopy. The sulfation reaction rate of condensed KCl is described by the following expressions: $dX/dt = 5.3 \times 10^{-3} \exp(-2120/T)(1-X)^{2/3}(C_{O_2})^{0.27}(C_{SO_2})^{0.27}(C_{H_2O})^{0.42}$ at 523–723 K and $dX/dt = 1.20 \times 10^4 \exp(-14180/T)(1-X)^{2/3}(C_{O_2})^{0.92}(C_{SO_2})^{0.39}(C_{H_2O})^{0.12}$ at 823–1023 K.

1. INTRODUCTION

Large amounts of alkali and chlorine in biomass fuels, which are more than those in fossil fuels, result in severe problems of slagging, fouling, and corrosion in heat exchangers of biomass-fired equipment.^{1,2} At high temperatures, alkali metals (e.g., K or Na), together with chlorine (Cl), are released from biomass into the flue gas as alkali metal chloride vapor.^{3–5} These species then undergo a series of condensation, nucleation, and agglomeration processes, which leads to slagging, fouling, and corrosion of heating surfaces. The chlorine species in the deposits would accelerate a high-temperature metal corrosion.^{6–8} Furthermore, some researchers have found that potassium chloride (KCl) can also make SCR catalysts deactivated, leading to a limited application of SCR for NO_x control in the biomass combustion system.^{9,10}

Compared with alkali chlorides, alkali sulfates have a rather high melting temperature that results in a lower deposition rate on the heating surface.^{11–13} Furthermore, alkali chlorides would react with chromium and deplete the protective oxide in chromium by forming alkali chromates, leading to severe corrosion. However, alkali sulfates would not.^{14–18} The sulfation process transforms alkali chlorides into alkali sulfates under the effects of sulfur species. This alkali transformation significantly relieves deposits, fouling, and corrosion on heat transfer surfaces during biomass combustion.

Most of the current investigations find that co-firing biomass fuels with coal (which has higher sulfur content than biomass),^{19–22} sulfur (S),²³ ammonium sulfate [(NH₄)₂SO₄],^{13,23–26} ferrous sulfate (FeSO₄), and ferrous sulfide (Fe₂S₂)^{20,27} decreases the deposition rate on heating surfaces to a certain degree. Co-firing biomass fuels with these elements also relieves the severe problems that occur in biomass-fired equipment. During biomass combustion, potassium and chloride are easily vaporized and released as KCl into

the flue gas. The gaseous KCl is then converted to K₂SO₄ through a homogeneous reaction with SO₂, O₂, and water vapor. Then, with the flue gas temperature decreasing, KCl exists as aerosol in flue gas because of condensation, and sulfation occurs. The KCl deposited on the heating surfaces can also be partially converted to K₂SO₄(s) through heterogeneous sulfation with SO₂, O₂, and water vapor in the flue gas.^{28–30} Figure 1 shows the homogeneous and heterogeneous sulfation processes of KCl during biomass combustion.

The detailed reaction mechanism and rate-limited elementary reaction of the homogeneous and heterogeneous alkali chloride sulfation are important in obtaining the alkali chloride–sulfate transformation mechanism and establishing a kinetic model. Limited research has been conducted on the KCl sulfation dynamics during biomass combustion, and previous studies on the sulfation of alkali chlorides mainly focused on gas turbine corrosion caused by NaCl.^{31–33} However, researchers have increasingly become interested in solving KCl-related problems during biomass combustion because of the considerable attention given to aerosol emissions and severe problems that occur in biomass-fired equipment. Iisa et al.³⁴ found a 100% homogeneous sulfation rate of KCl in a laminar entrained flow reactor. Glarborg and Marshall³⁵ proposed a sulfation mechanism of alkali chlorides and predicted alkali migration, which was confirmed by experiments conducted by Jimenez.³⁶ Hindiyarti et al.² developed and improved the sulfation mechanism to predict chlorine and sulfur migration in biomass co-fired with (NH₄)₂SO₄ and Al₂(SO₄)₃.²⁷ They observed that the sulfation rate depended on the formation of alkali sulfate aerosol. In addition, only a few investigations on the kinetic

Received: September 10, 2014

Revised: November 25, 2014

Published: November 30, 2014



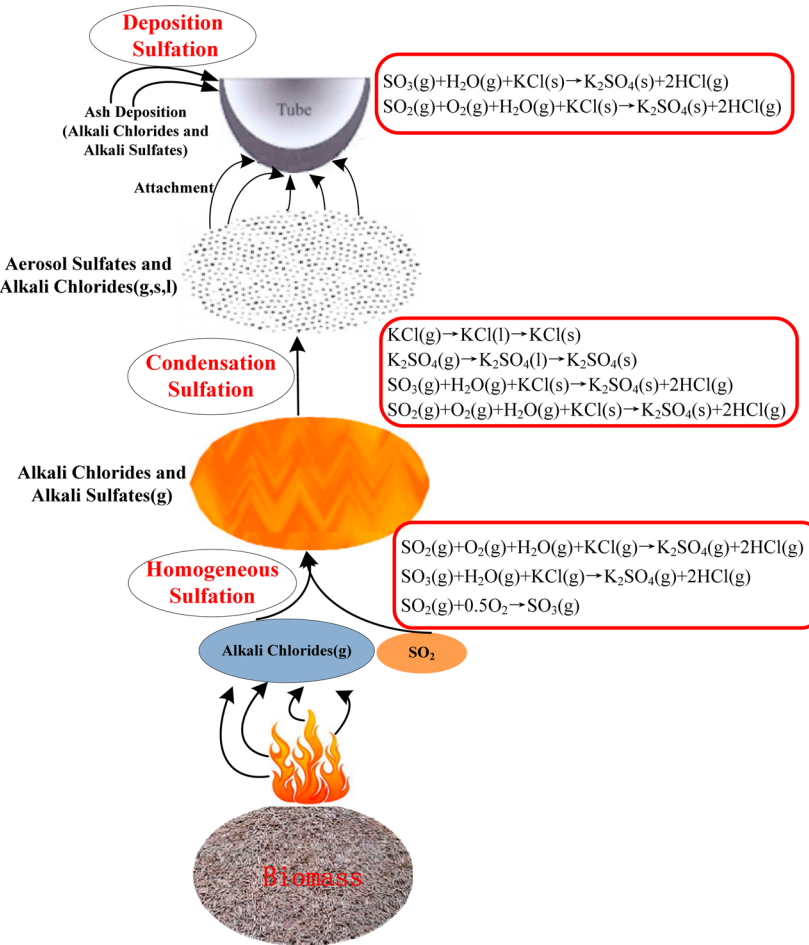


Figure 1. Migration mechanism of potassium deposition on a heating surface during biomass combustion.

sulfation of condensed KCl were conducted because of the difficulty in obtaining homogeneous sulfation data.

Matsuda et al.³² investigated the effects of sulfation temperature and reactant concentrations on the heterogeneous sulfation of NaCl, KCl, and CaCl₂ in a fixed-bed reactor. They found different sulfation kinetics mechanism of alkali and alkaline metal chlorides between high and low temperatures. Moreover, the heterogeneous sulfation rate expressions were established. However, Henriksson et al.³¹ found the lowest sulfation rate at 773 K in the heterogeneous NaCl sulfation, which was not observed in the experiments of Matsuda et al. Subsequently, the important events after a transition were investigated. Sengeløv et al.³⁷ studied the effects of temperature and reactant concentrations on the condensed KCl sulfation. Accordingly, an intermediate (i.e., potassium pyrosulfate (K₂S₂O₇)) or a eutectic formation at high temperatures might be generated. Thus, a two-stage distribution of reaction kinetics and a rate expression within the 823–1023 K range were observed. The researchers, however, failed to further analyze the sulfation at low temperatures. Studies on the reaction kinetics and differences within a wider temperature range were insufficient and unconsolidated.

This paper aims to study the heterogeneous sulfation rate of condensed KCl in a fixed-bed reactor during biomass combustion at a temperature range of 523–1023 K. The effects of sulfation temperature and reactant concentrations (SO₂/O₂/H₂O) are further considered. The sulfation rate is determined by measuring the sulfur content in solid residues. A rate expression

of the heterogeneous KCl sulfation is obtained after a kinetic analysis. The reaction mechanism difference at different temperature ranges is also discussed.

2. EXPERIMENTS AND METHODS

2.1. Fixed-Bed Reaction System. Solid KCl was placed on a porous plate in the isothermal zone of a fixed-bed quartz reactor. A schematic of the fixed-bed system is shown in Figure 2. Water vapor was generated using a peristaltic pump and an electric stove. This water vapor was then introduced into the reactor with a reactant gas (O₂), and SO₂ was introduced into the reactor with a balance gas (N₂). To avoid gas reactions before the solid layer, O₂ was through the outer tube while SO₂ was through the inner tube, and the mixing position was located at the bottom of the inner tube or above the KCl layer. The reactor temperature was measured under inert conditions with a type K thermocouple (accuracy ± 1 K). The emitted tail gas was then immersed in a sodium hydroxide solution. The KCl sample with 99.9% purity was ground and sieved to obtain a 100–200 μm size range. Each test used 1 g of sample material.

The KCl sample was then exposed to N₂ for 15 min and heated to the desired temperature under inert atmosphere. Then, N₂ was replaced with a mixture of SO₂, O₂, H₂O, and N₂ with total gas flow of 1 L/min in standard temperature and pressure. After a certain sulfation period, the solid products were cooled at room temperature in a nitrogen atmosphere. Subsequently, the product was collected and analyzed.

2.2. Test Methods. X-ray fluorescence (XRF, S4 PIONEER, Germany) was used to measure the total content of each element. Scanning electron microscopy–electron dispersive X-ray spectroscopy (SEM–EDX, JEOL JSM-6390A, Japan) was employed to determine

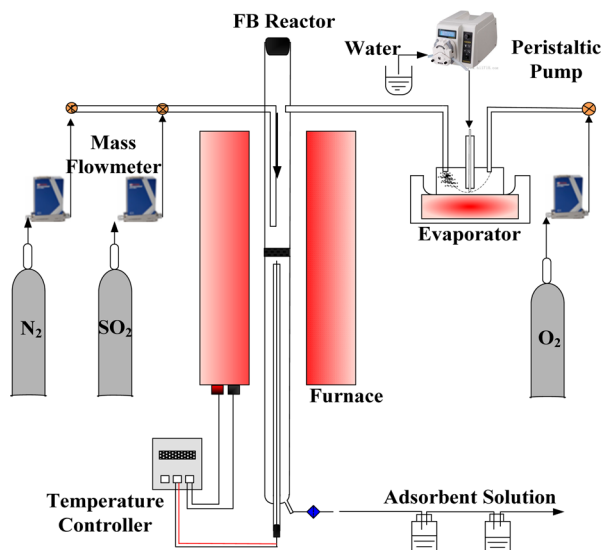


Figure 2. Schematic of the fixed-bed reactor.

the microstructure and elemental content distribution of the products. X-ray diffraction (XRD, X'pert MPD Pro, PANalytical, Netherlands) was used to analyze the potential mineral forms of alkali metals.

Figure 3 shows the effect of residence time on the sulfur content of the products. The sulfur contents approximately and linearly increased

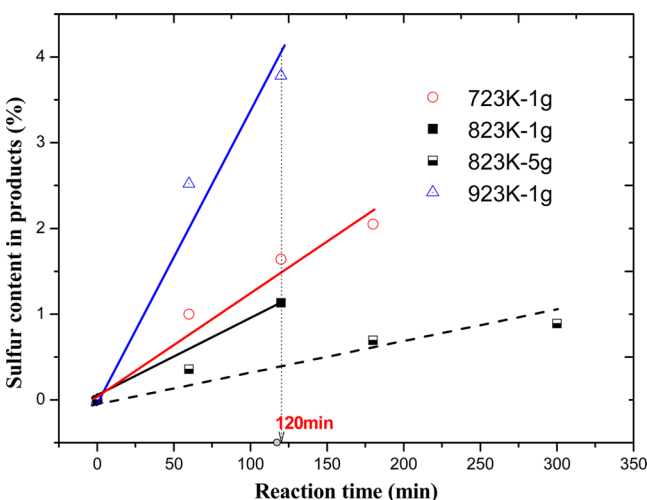


Figure 3. Time-effect validation at different experimental conditions (1% SO₂, 5% O₂, and 10% H₂O).

with the reaction time increase under different conditions. The KCl sulfation rate remained almost unchanged with the reaction time changing. Thus, the residence time for the experiments was set to 120 min to facilitate the subsequent dynamic analysis and calculation.

2.3. Kinetic Analysis Methods. The reaction rate is defined as dX/dt , where X is the KCl sulfation ratio determined by the sulfur content of the solid residuals. With the assumption of a shrinking core model, similar to the conditions presented by Matsuda et al.³² and Sengelov et al.,³⁷ dX/dt for different experimental conditions is determined by eq 1 as follows:

$$\frac{dX}{dt} = k(1 - X)^{2/3} C_{SO_2}^\alpha C_{O_2}^\beta C_{H_2O}^\gamma \quad (1)$$

where the reaction rate constant k in Arrhenius form denotes the temperature dependence; C_i is the concentration, where i represents the reactant gases; and α , β , and γ are the reaction series of different gases.

According to the Arrhenius formula, eq 2 defines the rate constant k as follows:

$$k = k_0 e^{-E/RT} \quad (2)$$

where E is the activation energy (kJ·mol⁻¹), R is the molar gas constant (8.314 J·mol⁻¹·K⁻¹), and k_0 is the frequency factor. Substituting k into eq 2, we can obtain the following equation:

$$\frac{dX}{dt} = k_0 e^{-E/RT} (1 - X)^{2/3} C_{SO_2}^\alpha C_{O_2}^\beta C_{H_2O}^\gamma \quad (3)$$

From eq 3, the formula can be simplified as follows:

$$\frac{d(1 - (1 - X)^{1/3})}{dt} = k'_0 e^{-E/RT} C_{SO_2}^\alpha C_{O_2}^\beta C_{H_2O}^\gamma \quad (4)$$

Then, the log of both sides of eq 4 can be rewritten as

$$\begin{aligned} \ln \frac{d(1 - (1 - X)^{1/3})}{dt} \\ = \ln k'_0 - \frac{E}{RT} + \alpha \ln C_{SO_2} + \beta \ln C_{O_2} + \gamma \ln C_{H_2O} \end{aligned} \quad (5)$$

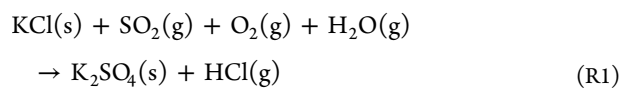
The activation energy (E) and the reaction order can be obtained from eq 5. For example, the activation energy (E) can be determined from the changing temperatures. Similarly, when we change the concentration of SO₂, O₂, or H₂O but keep the other parameters unchanged, the values α , β , and γ can be obtained from the linear fitting of the effect of the corresponding reactant concentration on the sulfation rate.

3. RESULTS AND DISCUSSION

3.1. Chemical Composition Determination by XRF and XRD.

The solid products were analyzed using XRF, and Figure 4 shows the element distribution under different conditions. Sulfur, oxide, chloride, and potassium were the main elements in the sulfation product of KCl, which indicated that SO₂ could be captured through the reaction with KCl in O₂ and water vapor environment. In Figure 4a, with increasing temperature, both sulfur and oxygen contents slowly increased below 723 K, slightly decreased when the temperature further increased to 823 K, and then sharply increased with the temperature increasing above 873 K. However, the change of potassium and chlorine contents with temperature was opposite to the change of sulfur and oxygen contents because of the capture on SO₂. In Figure 4b, we removed water vapor or O₂ at 723 and 923 K, respectively, and found the content of sulfur in the products was significantly reduced after water vapor or O₂ removal. It indicated that the reactants (e.g., O₂ and water vapor) were important to KCl sulfation. Moreover, if we compared the content of sulfur and oxygen content in Figure 4, it was found that sulfur content is low while oxygen content can be still high under certain conditions. This indicated that there should be remarkable adsorption of water vapor and O₂ occurring on the surfaces of solid particles.

XRD was used to analyze the products. Figure 5 shows the XRD patterns of the products at different temperatures. Only KCl and K₂SO₄ were found in the products; this result would suggest that only K₂SO₄ was the heterogeneous sulfated product of KCl, which was in accordance with the findings of Sengelov et al.³⁷ The following reaction R1 has been widely used to describe the sulfation process of KCl to produce K₂SO₄ and HCl in the atmosphere of SO₂, H₂O, and O₂.



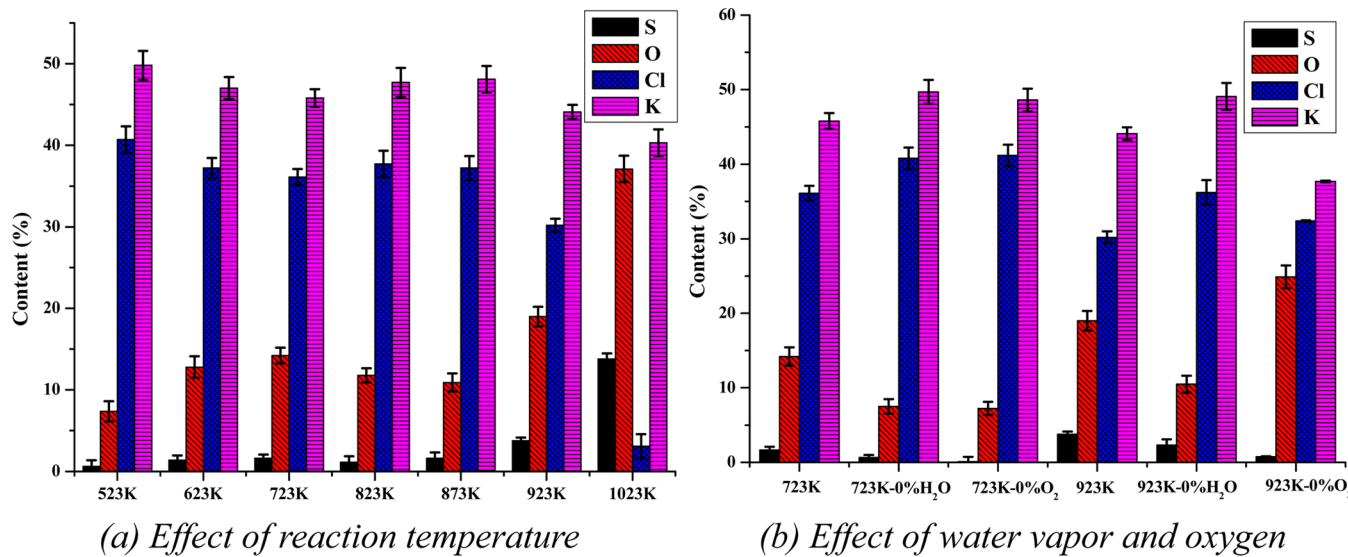


Figure 4. XRF element distributions of the solid products (1% SO₂, 5% O₂, 10% H₂O).

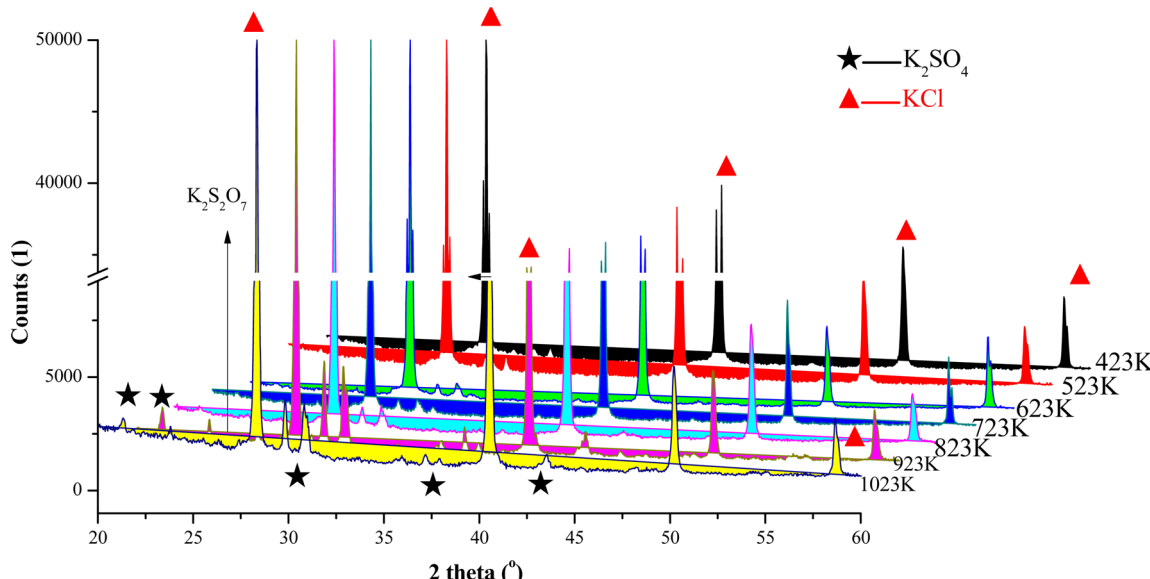
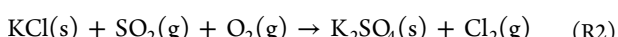


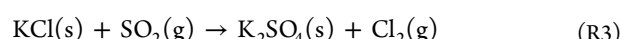
Figure 5. XRD patterns of products (1% SO₂, 5% O₂, and 10% H₂O).

However, note that in Figure 4b under the conditions without O₂ or water vapor, the content of sulfur was not zero, which indicated there should be other sulfation reaction routes besides R1. When the (10%) water vapor was removed, the sulfur content decreased from 1.64 to 0.678% at 723 K and from 3.78 to 2.34% at 923 K. It proved that KCl was still able to directly react with SO₂ and O₂ without water vapor to produce K₂SO₄ and Cl₂, which has been mentioned in previous works on chlorine corrosion in a biomass furnace as the following reaction R2.^{38,39}

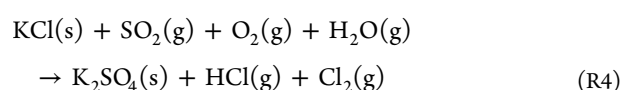


While (5%) O₂ was removed in Figure 4b, the sulfur content decreased from 1.64 to 0.104% at 723 K and from 3.78 to 0.784% at 923 K. The sulfur content under the condition without O₂ was lower than that without H₂O. It indicated that O₂ was more important than H₂O in the overall sulfation process of KCl. Because there was still a little sulfur detected, a

very weak reaction routine R3 proposed by Abdul Hye³⁹ and Riedl et al.⁴⁰ might exist.



Including the reaction conditions without O₂ or water vapor, in this study, the overall heterogeneous sulfation of solid KCl was proposed to be expressed by the following reaction R4:



3.2. Effect of Sulfation Temperature. 3.2.1. Sulfation Ratio and Arrhenius Plot. Figure 6 illustrates the effect of reaction temperature on the heterogeneous sulfation ratio under different conditions. This effect can be divided into three stages at different temperatures for conditions 1–4. First, the heterogeneous sulfation ratio slowly increased as the temperature increased from 523 to 723 K. The ratio decreased to its lowest value when the temperature was up to 823 K. However,

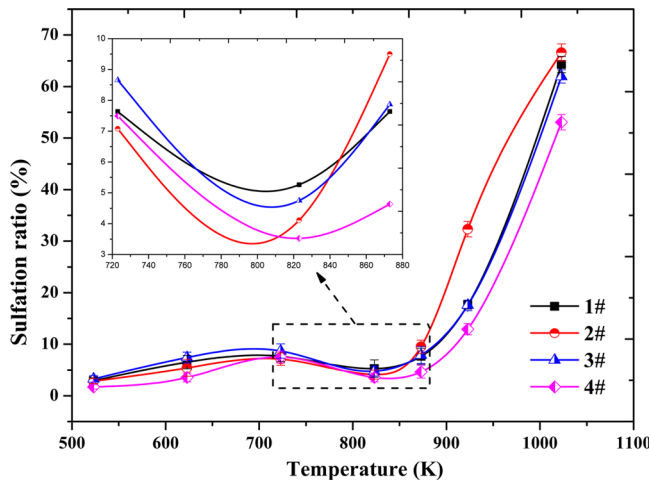


Figure 6. Temperature change of the sulfation ratio of KCl at different conditions (#1: 1% SO₂, 5% O₂, and 10% H₂O; #2: 1% SO₂, 10% O₂, and 10% H₂O; #3: 1% SO₂, 5% O₂, and 15% H₂O; #4: 0.5% SO₂, 5% O₂, and 10% H₂O).

the sulfation ratio began to increase rapidly and exponentially with the further increase of temperature. The sulfation ratio at high temperatures was significantly larger than that at low temperatures. Henriksson et al.³¹ investigated the heterogeneous NaCl sulfation in a fixed-bed reactor. KCl and NaCl were alkali metal chlorides with similar physical and chemical properties. Thus, a three-stage distribution in the sulfation rate and the lowest value at around the 773 K temperature were observed. Sengeløv et al.³⁷ and Matsuda et al.³² also studied the condensed KCl sulfation and found a considerably faster sulfation rate at high temperatures over 823 K. However, this sulfation rate was relatively slow below 823 K, which was consistent with the data of the present study.

On the basis of the previous experiments, the kinetic analysis of KCl sulfation was conducted. Figure 7 shows the Arrhenius plot of the sulfation reaction at different experimental conditions as well as the comparison between this study and the literature data.^{32,37} A change in the sulfation reaction mechanism between temperatures of 723 and 823 K evidently occurred in accordance with the results of previous studies.^{32,37} The activation energy

for the high-temperature mechanism was determined as 106–130 kJ·mol⁻¹, which agreed with the 137 kJ·mol⁻¹ reported by Matsuda et al.³² but was slightly lower than the 157 kJ·mol⁻¹ obtained by Sengeløv et al.³⁷ The activation energy for the low-temperature mechanism was determined as 15–23 kJ·mol⁻¹, which matched the 17 kJ·mol⁻¹ value observed by Matsuda et al.³²

The reason for the observed three-stage distribution and change in mechanism is still unclear. Some studies suggested that K₂S₂O₇ dominated the sulfation product at low temperatures. Under these conditions, K₂S₂O₇ was thermodynamically favored more than K₂SO₄.^{37,41} The formation of K₂S₂O₇ was exothermic. When the temperature was increased to 823 K or more, K₂S₂O₇ would decompose, which is endothermic. However, there are also some studies concluding that a phase transition occurs at high temperatures.^{32,37,42} The sulfation at low temperatures may involve a condensed-phase intermediate, perhaps a potassium sulfite. In fact, at low temperatures, K₂S₂O₇ was not found in the sulfation products (Figure 5). Therefore, the reason should be ascribed to a phase transition and the formation of a eutectic involved at high temperatures.

3.2.2. SEM. SEM was used to measure the product morphology at different temperatures, as shown in Figure 8. At a low reaction temperature of 723 K, the morphology of the solid products in Figure 8b was unchanged compared with that of the raw material in Figure 8a. However, as shown in Figure 8c, KCl and its product have partially melted at a higher temperature of 823 K because of the eutectic formation. An obvious molten phenomenon was observed at 923 K temperature, as shown in Figure 8d. The sulfation rate increase below 723 K was mainly due to the temperature increase. At a higher temperature (823 K), a mixture of KCl and generated K₂SO₄ began to melt, thereby dramatically decreasing the surface area between the solid KCl and the reactant gases and leading to a slight decline in the sulfation rate. With the temperature further increasing, KCl and generated K₂SO₄ formed a eutectic, and some KCl vaporized, making a change in the reaction mode from a gas–solid to a gas–liquid and/or a gas phase reaction³² that led to a rapid sulfation rate. Consequently, the three-stage distribution and high–low temperature mechanism difference were mainly due to the eutectic formation that resulted in the phase transition.

3.3. Effect of Reactant Concentrations. The effects of reactant concentrations (O₂, H₂O, and SO₂) on the KCl sulfation were also investigated. Figure 9 shows the influence of the O₂ concentration on the heterogeneous KCl sulfation. The sulfation ratio of KCl at a high temperature (923 K) increased linearly with the O₂ concentration within the 0–10% range, as shown in Figure 9a, while the sulfation ratio at a low temperature (723 K) increased with the O₂ concentration below 5% and remained unchanged thereafter. Figure 9b presents the kinetic analysis of a linear regression for the 2.5–10% O₂ concentration range. The reaction order for O₂ was significantly different between low and high temperatures with orders of 0.27 and 0.92, respectively. The O₂ effect at high temperatures was much more significant than that at low temperatures, which would indicate that the sulfation at high temperatures might be dominated by the O₂(g) → O₂(ads) adsorption reaction. The reaction order obtained at low temperatures matched that of the 0.3 value reported by Matsuda et al.³²

Figure 10 presents the SO₂ effect on the KCl sulfation. The sulfation ratio increased within the 0–0.5% range and remained

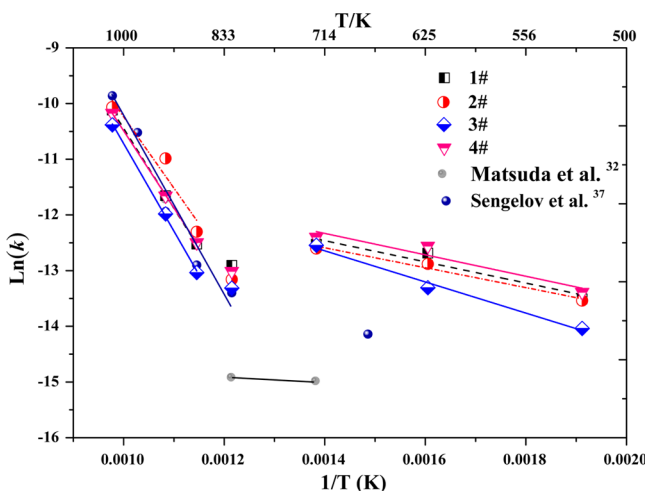


Figure 7. Arrhenius plot for the rate constant of KCl sulfation and comparison of current results with previous studies.

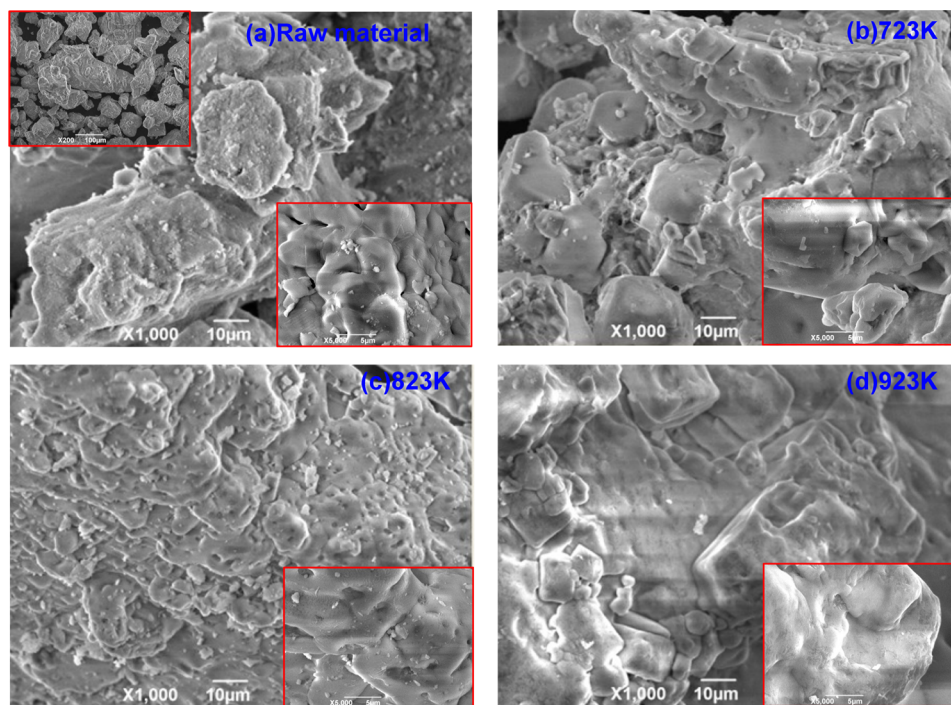


Figure 8. Microstructure of products at different temperatures (1% SO₂, 5% O₂, and 10% H₂O).

unchanged thereafter at 723 and 923 K. Considering the SO₂ emission within 1000 ppm during biomass combustion, the SO₂ concentration should significantly affect the sulfation rate. The reaction orders at the low and high temperatures were 0.27 and 0.39, respectively, as shown in Figure 10b. The values obtained at the low temperatures over a large SO₂ concentration range (0.1–2%) agreed with the 0.2 value obtained by Matsuda et al.³² for the 0.3–1.3% SO₂ concentration range. However, the values obtained at the high temperatures were slightly lower than the 0.59 and 0.5 values reported by Sengelov et al.³⁷ and Matsuda et al.,³² respectively.

Figure 11 shows the results of changing the water vapor concentration within the 5–15% range. The KCl sulfation ratio increased with the H₂O concentration increase below 8%. However, the value remained unchanged at a high temperature (923 K). The ratio approximately increased linearly with water vapor concentration at a low temperature (723 K). The reaction orders were 0.42 at low temperatures but lower with 0.12 at high temperatures. It seemed that the KCl sulfation rate was almost independent of water vapor concentration at high temperatures. However, at low temperatures, the effect of the water vapor was still important. The present reaction order of 0.12 at high temperatures agreed with the 0.15 value reported by Sengelov et al.³⁷

Based on the preceding experimental data, the sulfation rate as a function of temperature (523–1023 K) and reactant concentrations was determined as follows:

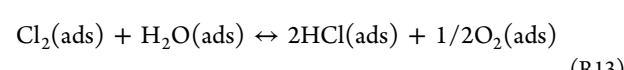
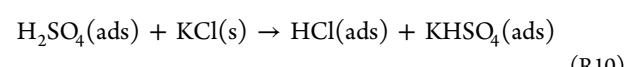
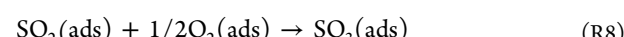
$$\frac{dX}{dt} = 5.32 \times 10^{-3} \exp^{-2120/T} (1 - X)^{2/3} C_{O_2}^{0.27} C_{SO_2}^{0.27} C_{H_2O}^{0.42}$$

$$523 \text{ K} < T < 723 \text{ K}$$

$$\frac{dX}{dt} = 1.20 \times 10^4 \exp^{-14186/T} (1 - X)^{2/3} C_{O_2}^{0.92} C_{SO_2}^{0.39} C_{H_2O}^{0.12}$$

$$823 \text{ K} < T < 1023 \text{ K}$$

3.4. Reaction Mechanisms on the KCl Sulfation. A KCl sulfation mechanism in the presence of SO₂, H₂O, and O₂, which is similar to that proposed by Henriksson and Warnqvist,³¹ Boonsongsup et al.,³³ Wei et al.,⁴³ and Adams et al.,⁴⁴ is presented as follows:



In the practical biomass-fired furnaces, the flue gas usually contains all the reactants like SO₂, H₂O, and O₂. Under this condition, as shown in Figure 12, the transformations of K, Cl, and S were mainly along the routes (the thickest lines) of R10–R11, R10/R11, and R6–R8–R9–R10–R11, respectively. The reactant gases (O₂(g), SO₂(g), and H₂O(g)) are first absorbed on the surface of the condensed KCl. Then, SO₂(ads) is converted into SO₃(ads) through oxidation with O₂(ads). Generated SO₃(ads) then reacts with H₂O(ads) and forms H₂SO₄(ads). Finally, the products K₂SO₄(s) and HCl(g) are obtained through a reaction between KCl(s) and an intermediate KHSO₄(ads).

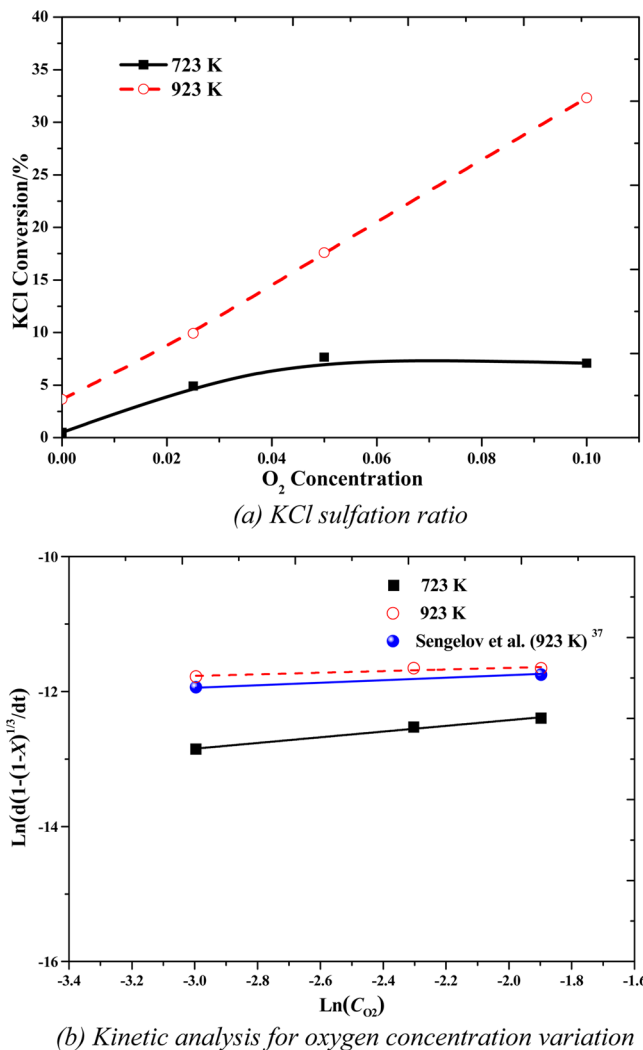


Figure 9. Results of the KCl sulfation for oxygen concentration variation (1% SO_2 , 5% O_2 , and 10% H_2O).

Under the conditions without water vapor, it was impossible to produce K_2SO_4 from KCl by the routine R10–R11. However, there was still a certain amount of sulfur in the products shown from Figure 4b and Figure 11a, as the mechanism proposed by Blomberg et al.,³⁸ KCl could still directly react with SO_2 and O_2 to produce K_2SO_4 and Cl_2 through reaction R2 in Figure 12. While under the conditions without O_2 , Figure 4b and Figure 9a showed that very little sulfur was detected, and this should be through the weak reaction routine R3 proposed by Abdul Hye³⁹ and Riedl et al.⁴⁰ in Figure 12.

Moreover, the experimental results showed that the apparent sulfation mechanism was significantly different between low and high temperatures. The sulfation rate dependence on the reactant concentrations at low temperatures indicated that all the reactants contributed to the heterogeneous sulfation. When we assumed that SO_2 and O_2 molecules adsorbed on two KCl phase surface sites,³¹ the same reaction order suggested that $\text{SO}_2(\text{ads})$ oxidation (R8) might be a rate-limiting step. As Henriksson and Warnqvist³¹ mentioned, H_2O was strongly adsorbed on the KCl phase surface,³¹ which meant a rapid R5 reaction rate. Furthermore, certain H_2O sulfation effects were observed. Consequently, R9 involved with $\text{H}_2\text{O}(\text{ads})$ might also be a rate-determining reaction. However, the O_2 reaction order with a value of nearly 1 at high temperatures was considerably

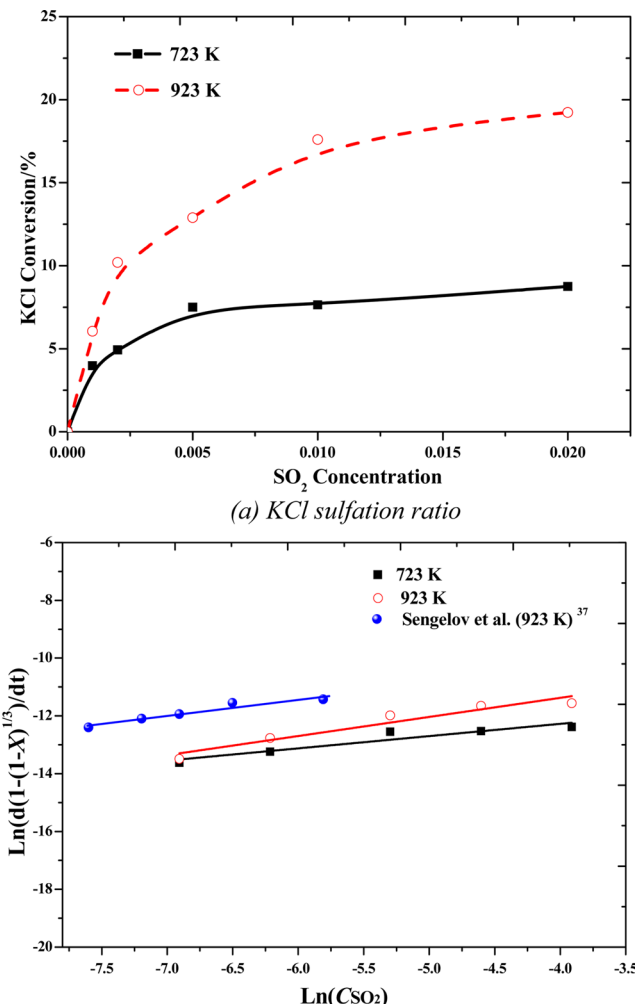


Figure 10. Results of the KCl sulfation for sulfur dioxide concentration variation (1% SO_2 , 5% O_2 , and 10% H_2O).

larger than that of water vapor and SO_2 . This result indicated that O_2 significantly influenced the sulfation rate, whereas water vapor and SO_2 did not. The combination of information above and the proposed mechanism showed that the KCl sulfation should be dominated by the O_2 absorption (R5).

4. CONCLUSIONS

Sulfation of condensed alkali chloride was conducted in a fixed-bed reactor at the 523–1023 K temperature range with reactant gases, namely, 0.1–2% SO_2 , 2.5–10% O_2 , and 5–15% H_2O . The following main conclusions are drawn:

(1) K_2SO_4 is the only sulfation product, and no other potassium sulfates are found. The KCl sulfation rate within the 523–1023 K temperature range is divided into three stages as follows: the sulfation rate slowly increases at the 523–723 K temperature range; the sulfation rate declines to the lowest value when the temperature is up to 823 K; and when the temperature is further increased, the sulfation rate rapidly and exponentially increases because of the eutectic formation at high temperatures that leads to a phase transition.

(2) The KCl sulfation rate increases linearly with the O_2 concentration ranging from 0 to 10% at a high temperature (923 K). While at a low temperature (723 K), the sulfation rate increases with the O_2 concentration below 5% and then is

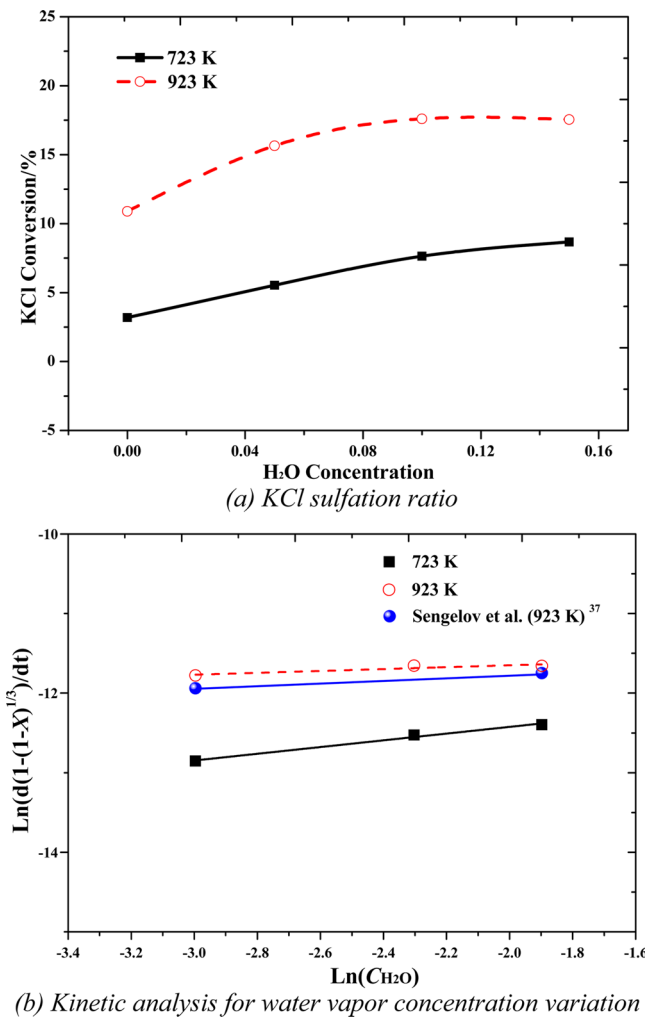


Figure 11. Results of the KCl sulfation for water vapor concentration variation (1% SO_2 , 5% O_2 , and 10% H_2O).

unchanged. The rate shows a similar tendency with SO_2 concentration to increase at 723 and 923 K, first increasing within the 0–0.5% range and then remaining unchanged. The sulfation rate increases with the H_2O concentration below 8% and then remains unchanged at a high temperature (923 K). At a low temperature (723 K), the sulfation rate increases linearly with water vapor concentration.

(3) A change in the sulfation reaction mechanism occurs within the 723–823 K temperature range. The sulfation rate of condensed KCl is described as $dX/dt = 5.32 \times 10^{-3} \exp(-2120/T)(1 - X)^{2/3}(C_{\text{O}_2})^{0.27}(C_{\text{SO}_2})^{0.27}(C_{\text{H}_2\text{O}})^{0.42}$ and $dX/dt = 1.20 \times 10^4 \exp(-14180/T)(1 - X)^{2/3}(C_{\text{O}_2})^{0.92}(C_{\text{SO}_2})^{0.39}(C_{\text{H}_2\text{O}})^{0.12}$ at 523–723 and 823–1023 K, respectively.

AUTHOR INFORMATION

Corresponding Author

*E-mail: wxb005@mail.xjtu.edu.cn. Telephone: +86-029-82668051. Facsimile: +86-029-82668703.

Notes

The authors declare no competing financial interest.

ACKNOWLEDGMENTS

This study was supported by the National Natural Science Foundation of China (Nos. 51306142 and 51376147). We also thank Peter Glarborg of the Technical University of Denmark for his assistance with the discussion of the sulfation experimental results.

REFERENCES

- Wei, X.; Schnell, U.; Hein, K. Behaviour of gaseous chlorine and alkali metals during biomass thermal utilisation. *Fuel* **2005**, *84*, 841–848.
- Hindiyarti, L.; Frandsen, F.; Livbjerg, H.; Glarborg, P.; Marshall, P. An exploratory study of alkali sulfate aerosol formation during biomass combustion. *Fuel* **2008**, *87*, 1591–1600.
- Silvennoinen, J.; Hedman, M. Co-firing of agricultural fuels in a full-scale fluidized bed boiler. *Fuel Process. Technol.* **2013**, *105*, 11–19.

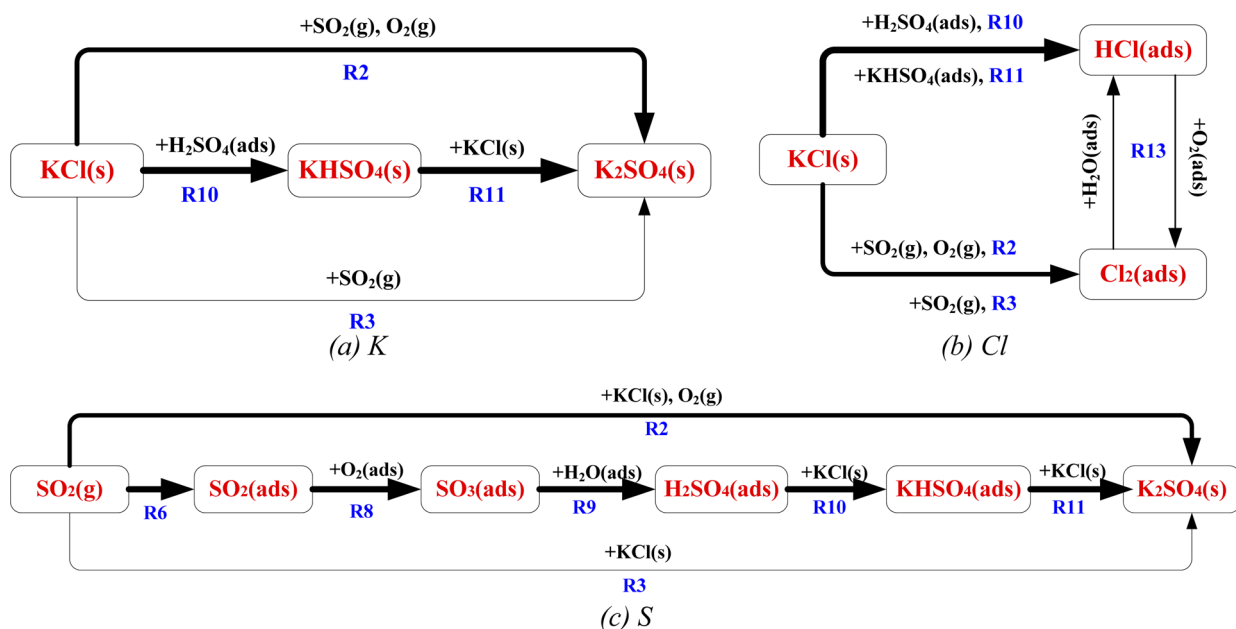


Figure 12. Reaction pathway of K, Cl, and S in the sulfation process.

- (4) Enestam, S.; Bankiewicz, D.; Tuiremo, J.; Mäkelä, K.; Hupa, M. Are NaCl and KCl equally corrosive on superheater materials of steam boilers? *Fuel* **2013**, *104*, 294–306.
- (5) Nielsen, H.; Frandsen, F.; Dam-Johansen, K.; Baxter, L. The implications of chlorine-associated corrosion on the operation of biomass-fired boilers. *Prog. Energy Combust. Sci.* **2000**, *26*, 283–298.
- (6) Davidsson, K. O.; Åmand, L. E.; Steenari, B. M.; Edled, A. L.; Eskilsson, D.; Leckner, B. Countermeasures against alkali-related problems during combustion of biomass in a circulating fluidized bed boiler. *Chem. Eng. Sci.* **2008**, *63*, 5314–5329.
- (7) Michelsen, H. P.; Frandsen, F.; Dam-Johansen, K.; Larsen, O. H. Deposition and high temperature corrosion in a 10 MW straw fired boiler. *Fuel Process. Technol.* **1998**, *54*, 95–108.
- (8) Bankiewicz, D.; Yrjas, P.; Hupa, M. High-temperature corrosion of superheater tube materials exposed to zinc salts. *Energy Fuels* **2009**, *23*, 3469–3474.
- (9) Benson, S. A.; Laumb, J. D.; Crocker, C. R.; Pavlish, J. H. SCR catalyst performance in flue gases derived from subbituminous and lignite coals. *Fuel Process. Technol.* **2005**, *86*, 577–613.
- (10) Kling, A.; Andersson, C.; Myringer, A.; Eskilsson, D.; Jaras, S. Alkali deactivation of high-dust SCR catalysts used for NOx reduction exposed to flue gas from 100MW-scale biofuel and peat fired boilers: influence of flue gas composition. *Appl. Catal. B* **2007**, *69*, 240–251.
- (11) Wang, L.; Hustad, J. E.; Skreiberg, Ø.; Skjevrek, G.; Grønli, M. A critical review on additives to reduce ash related operation problems in biomass combustion applications. *Energy Procedia* **2012**, *20*, 20–29.
- (12) Aho, M.; Vainikka, P.; Taipale, R.; Yrjas, P. Effective new chemicals to prevent corrosion due to chlorine in power plant superheaters. *Fuel* **2008**, *87*, 647–654.
- (13) Broström, M.; Kassman, H.; Helgesson, A.; Berg, M.; Andersson, C.; Backman, R.; Nordin, A. Sulfation of corrosive alkali chlorides by ammonium sulfate in a biomass fired CFB boiler. *Fuel Process. Technol.* **2007**, *88*, 1171–1177.
- (14) Karlsson, S.; Jonsson, T.; Hall, J.; Svensson, J.-E.; Liske, J. Mitigation of fireside corrosion of stainless steel in power plants: a laboratory study of the influences of SO₂ and KCl on initial stages of corrosion. *Energy Fuels* **2014**, *28*, 3102–3109.
- (15) Paneru, M.; Stein-Brzozowska, G.; Maier, J. r.; Scheffknecht, G. N. Corrosion mechanism of alloy 310 austenitic steel beneath NaCl deposit under varying SO₂ concentrations in an oxy-fuel combustion atmosphere. *Energy Fuels* **2013**, *27*, 5699–5705.
- (16) Pettersson, J.; Folkeson, N.; Johansson, L.-G.; Svensson, J.-E. The effects of KCl, K₂SO₄ and K₂CO₃ on the high temperature corrosion of a 304-type austenitic stainless steel. *Oxid. Met.* **2011**, *76*, 93–109.
- (17) Pettersson, C.; Pettersson, J.; Asteman, H.; Svensson, J.-E.; Johansson, L.-G. KCl-induced high temperature corrosion of the austenitic Fe–Cr–Ni alloys 304L and Sanicro 28 at 600 °C. *Corros. Sci.* **2006**, *48*, 1368–1378.
- (18) Hiramatsu, N.; Uematsu, Y.; Tanaka, T.; Kinugasa, M. Effects of alloying elements on NaCl-induced hot corrosion of stainless steels. *Mater. Sci. Eng., A* **1989**, *120*, 319–328.
- (19) Kassman, H.; Broström, M.; Berg, M.; Åmand, L.-E. Measures to reduce chlorine in deposits: application in a large-scale circulating fluidised bed boiler firing biomass. *Fuel* **2011**, *90*, 1325–1334.
- (20) Yang, T.; Kai, X.; Sun, Y.; He, Y.; Li, R. The effect of coal sulfur on the behavior of alkali metals during co-firing biomass and coal. *Fuel* **2011**, *90*, 2454–2460.
- (21) Robinson, A. L.; Junker, H.; Baxter, L. L. Pilot-scale investigation of the influence of coal-biomass cofiring on ash deposition. *Energy Fuels* **2002**, *16*, 343–355.
- (22) Theis, M.; Skrifvars, B.-J.; Zevenhoven, M.; Hupa, M.; Tran, H. Fouling tendency of ash resulting from burning mixtures of biofuels. Part 3. Influence of probe surface temperature. *Fuel* **2006**, *85*, 2002–2011.
- (23) Kassman, H.; Bäfver, L.; Åmand, L.-E. The importance of SO₂ and SO₃ for sulphation of gaseous KCl—an experimental investigation in a biomass fired CFB boiler. *Combust. Flame* **2010**, *157*, 1649–1657.
- (24) Henderson, P.; Szakálos, P.; Pettersson, R.; Andersson, C.; Höglberg, J. Reducing superheater corrosion in wood-fired boilers. *Mater. Corros.* **2006**, *57*, 128–134.
- (25) Kassman, H.; Pettersson, J.; Steenari, B.-M.; Åmand, L.-E. Two strategies to reduce gaseous KCl and chlorine in deposits during biomass combustion—addition of ammonium sulphate and co-combustion with peat. *Fuel Process. Technol.* **2013**, *105*, 170–180.
- (26) Kassman, H. Strategies to reduce gaseous KCl and chlorine in deposits during combustion of biomass in fluidised bed boilers. Ph.D. Thesis, Chalmers University of Technology, 2012.
- (27) Wu, H.; Pedersen, M. N.; Jespersen, J. B.; Aho, M.; Roppo, J.; Frandsen, F. J.; Glarborg, P. Modeling the use of sulfate additives for potassium chloride destruction in biomass combustion. *Energy Fuels* **2014**, *28*, 199–207.
- (28) Christensen, K. A.; Stenholm, M.; Livbjerg, H. The formation of submicron aerosol particles, HCl and SO₂ in straw-fired boilers. *J. Aerosol Sci.* **1998**, *29*, 421–444.
- (29) Christensen, K. A. Formation of submicron particles from the combustion of straw. *J. Aerosol Sci.* **1995**, *26*, 691.
- (30) Kaufmann, H. Chlorine-compounds in emissions and residues from the combustion of herbaceous biomass. Ph.D. Thesis, Swiss Federal Institute of Technology Zürich, 1997.
- (31) Henriksson, M.; Warnqvist, B. Kinetics of formation of HCl (g) by the reaction between NaCl (s) and SO₂, O₂, and H₂O (g). *Ind. Eng. Chem. Process Des. Dev.* **1979**, *18*, 249–254.
- (32) Matsuda, H.; Ozawa, S.; Naruse, K.; Ito, K.; Kojima, Y.; Yanase, T. Kinetics of HCl emission from inorganic chlorides in simulated municipal wastes incineration conditions. *Chem. Eng. Sci.* **2005**, *60*, 545–552.
- (33) Boonsongsup, L.; Iisa, K.; Frederick, W. Kinetics of the sulfation of NaCl at combustion conditions. *Ind. Eng. Chem. Res.* **1997**, *36*, 4212–4216.
- (34) Iisa, K.; Lu, Y.; Salmenoja, K. Sulfation of potassium chloride at combustion conditions. *Energy Fuels* **1999**, *13*, 1184–1190.
- (35) Glarborg, P.; Marshall, P. Mechanism and modeling of the formation of gaseous alkali sulfates. *Combust. Flame* **2005**, *141*, 22–39.
- (36) Jiménez, S.; Ballester, J. Formation of alkali sulphate aerosols in biomass combustion. *Fuel* **2007**, *86*, 486–493.
- (37) Sengelov, L. W.; Hansen, T. B.; Bartolomé, C.; Wu, H.; Pedersen, K. H.; Frandsen, F. J.; Jensen, A. D.; Glarborg, P. Sulfation of condensed potassium chloride by SO₂. *Energy Fuels* **2013**, *27*, 3283–3289.
- (38) Blomberg, T. Which are the right test conditions for the simulation of high temperature alkali corrosion in biomass combustion? *Mater. Corros.* **2006**, *57*, 170–175.
- (39) Abdul Hye, A. S. M. Computational fluid dynamics (CFD) study of co-firing of coal and pretreated biomass. Ph.D. Thesis, KTH Industrial Engineering and Management, Stockholm, Sweden, 2014.
- (40) Riedl, R.; Dahl, J.; Obernberger, I.; Narodoslawsky, M. Corrosion in fire tube boilers of biomass combustion plants. In *Proceedings of the China International Corrosion Control Conference*, 1999.
- (41) Lindberg, D.; Backman, R.; Hupa, M.; Chartrand, P. Thermodynamic evaluation and optimization of the (Na + K + S) system. *J. Chem. Thermodyn.* **2006**, *38*, 900–915.
- (42) Ozawa, S.; Naruse, K.; Ito, K.; Kojima, Y.; Matsuda, H.; Mishima, S.-i.; Endo, M.; Yanase, T. Evolution of HCl from KCl, CaCl₂ and NaCl in an SO₂-O₂-H₂O atmosphere under a simulated condition of municipal wastes incineration. *J. Chem. Eng. Jpn.* **2003**, *36*, 867–873.
- (43) Wei, X.; Lopez, C.; Von Puttkamer, T.; Schnell, U.; Unterberger, S.; Hein, K. R. Release of chlorine and its retention in ash during co-combustion of biomass and coal in a pulverized fuel combustor. *Int. J. Energy Clean Environ.* **2004**, DOI: 10.1615/InterJenerCleanEnv.v5.i1.10.
- (44) Adams, B.; Diederen, H. S.; Peeters, K.; Wijnhoven, J. P.; Eeraerts, D. In Seghers Boiler Prism: A Proven Primary Measure against High Temperature Boiler Corrosion. In *12th Annual North American Waste-to-Energy Conference*; American Society of Mechanical Engineers, 2004; pp 229–240.